

# Spectroscopy of 1.55 $\mu\text{m}$ PbS quantum dots on Si photonic crystal cavities with a fiber taper waveguide

M. T. Rakher,<sup>1,a)</sup> R. Bose,<sup>2,b)</sup> C. W. Wong,<sup>2</sup> and K. Srinivasan<sup>1</sup>

<sup>1</sup>Center for Nanoscale Science and Technology, National Institute of Standards and Technology, Gaithersburg, Maryland 20899, USA

<sup>2</sup>Optical Nanostructures Laboratory, Center for Integrated Science and Engineering, Solid-State Science and Engineering, and Mechanical Engineering, Columbia University, New York, New York 10027, USA

(Received 7 December 2009; accepted 26 March 2010; published online 23 April 2010)

We use an optical fiber taper waveguide to probe PbS quantum dots (QDs) dried on Si photonic crystal cavities near 1.55  $\mu\text{m}$ . We demonstrate that a low density ( $\leq 100 \mu\text{m}^{-2}$ ) of QDs does not significantly degrade cavity quality factors as high as  $\approx 3 \times 10^4$ . We also show that the tapered fiber can be used to excite the QDs and collect the subsequent cavity-filtered photoluminescence, and present measurements of reversible photodarkening and QD saturation. This method represents an important step toward spectroscopy of single colloidal QDs in the telecommunications band. © 2010 American Institute of Physics. [doi:10.1063/1.3396988]

The combination of low optical absorption and mature device processing has resulted in the development of low loss silicon photonic devices such as high quality factor ( $Q$ ) photonic crystal cavities (PCCs) operating in the technologically relevant 1.55  $\mu\text{m}$  wavelength range.<sup>1–3</sup> Silicon's indirect band gap represents a challenge in making light-emitting devices and as a result there has been considerable interest in developing hybrid systems integrating a light-emitting material.<sup>4,5</sup> Lead salt colloidal quantum dots<sup>6</sup> (QDs) represent one such approach. In addition, their atomiclike properties suggest the potential for Si-based quantum information processing in the single QD limit. In this work, we use colloidal PbS QDs as the active material to interact with Si PCCs with resonances near 1.55  $\mu\text{m}$ . Due to the long radiative lifetime [ $\approx 700$  ns (Refs. 7 and 8)] and small radiative efficiency of these dried QDs [ $\approx 1\%$  (Refs. 7 and 9)], as well as challenges associated with measuring low light levels with InGaAs detectors,<sup>10</sup> it is of the utmost importance to collect as many emitted photons as possible. Previous studies of PbS/PbSe QDs coupled to Si microcavities<sup>11–14</sup> have relied on free-space microphotoluminescence methods to pump and collect the emission from moderately high- $Q$  cavities ( $Q \approx 10^3$ ), and have generally operated at relatively high QD densities, or else have sacrificed spectral resolution to achieve the count rates needed to operate at a lower QD density.<sup>15</sup> In this work, we use an optical fiber taper waveguide<sup>2,16</sup> to couple to the modes of high- $Q$  PCCs ( $Q \approx 10^4$ ), thereby allowing for an efficient out-coupling mechanism for PbS QD emission. We measure photoluminescence (PL) from a low density ( $\leq 100 \mu\text{m}^{-2}$ ) of spun QDs and show that the  $Q$  does not degrade due to QD absorption up to  $Q \approx 3 \times 10^4$ . We also measure photodarkening and saturation of the QD emission into the cavity mode. This approach may enable the future interrogation of cavity quantum electrodynamics (cQED) in the PbS/Si system, in much the same way as has been demonstrated for epitaxial III-V QDs.<sup>17</sup>

The PbS QDs (Ref. 18) are chemically synthesized<sup>19</sup> and suspended in chloroform. As shown in the inset of Fig. 2(a), the emission is centered near 1460 nm with a width of 100 nm due to a combination of size inhomogeneities and a large homogeneous linewidth at room temperature. The solution is further diluted with chloroform in a 1:200 mixture. Approximately 20  $\mu\text{L}$  is spin-coated directly onto the substrate containing PCCs, yielding an areal density of  $\leq 100 \mu\text{m}^{-2}$  [inset of Fig. 1(g)] as measured by a scanning electron microscope (SEM). The PCCs measured [Figs. 1(a)–1(c)] are the well-developed H1,<sup>20</sup> L3,<sup>1</sup> and multiheterostructure (MH) cavities,<sup>3</sup> and have been fabricated in a 250 nm thick Si device layer using standard silicon-on-insulator fabrication methods. The devices are probed using an optical fiber taper waveguide, which can be used to measure the spectral response of the devices in transmission as well to collect PL.

Transmission measurements follow the approach of Ref. 2, where light from a swept wavelength external cavity diode

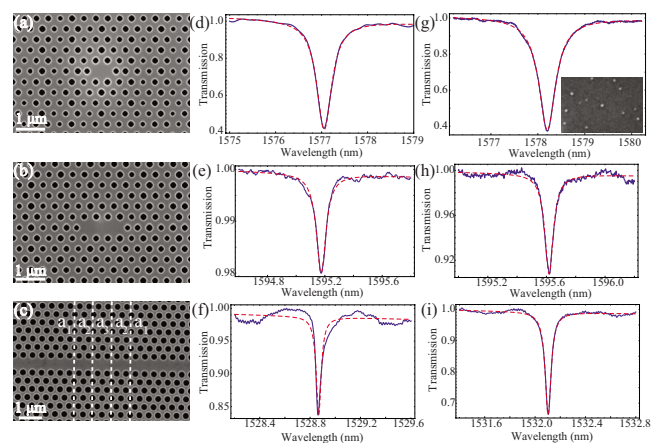


FIG. 1. (Color online) [(a)–(c)] SEM images of the H1, L3, and MH cavities, respectively. The lattice constants in (c) are  $\{a_1, a_2, a_3\} = \{410 \text{ nm}, 415 \text{ nm}, 420 \text{ nm}\}$ . [(d)–(f)] Transmission spectrum of the H1, L3, and MH cavities before QD spin with fits (dashed). (d) and (f) were taken with the taper in contact with the cavity, while (e) was taken with the taper above the cavity. [(g)–(i)] Same as [(d)–(f)] but after QD spin. Inset of (g) SEM image of QDs in a  $256 \times 173 \text{ nm}^2$  area.

<sup>a)</sup>Electronic mail: mrakher@nist.gov.

<sup>b)</sup>Present address: Institute for Research in Electronics and Applied Physics, University of Maryland, College Park, MD 20742, USA.

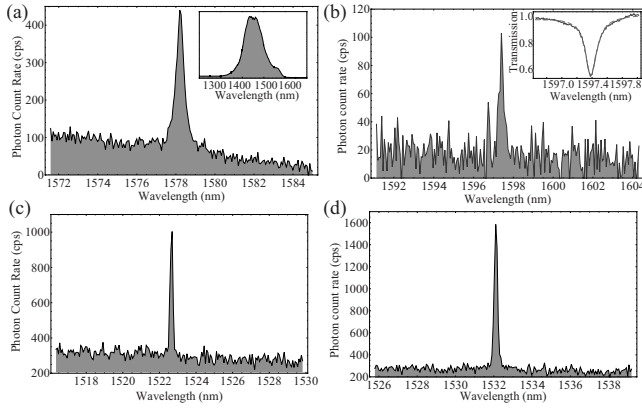


FIG. 2. (Color online) Fiber-collected PL spectra for (a) H1, (b) L3, and [(c)–(d)] MH PCCs. Inset of (a) Room-temperature PL of an ensemble of QDs without cavity. Inset of (b) L3 transmission with taper in contact with cavity.

laser (1520 to 1630 nm) is sent through a variable optical attenuator and polarization controller before it is directed through the tapered optical fiber to an InGaAs photodiode. The taper and sample separation is controlled via  $x$ ,  $y$ , and  $z$  stepper stages with 50 nm resolution, and the system is imaged under a  $50\times$  microscope objective. The measurement setup rests in a  $N_2$ -rich environment at room temperature to prevent irreversible photooxidation of the QDs (Ref. 21) and taper degradation.

This technique enables resonant spectroscopy of the cavity with and without the active material. In this way, we measured the cavity  $Q$ , before and after addition of the PbS QDs. Figures 1(d)–1(f) show a resonance of the H1, L3, and MH cavities in transmission without QDs, with measured  $Q$ s as high as 27 400. The extracted  $Q_{i+p}$  values, which include intrinsic and parasitic losses,<sup>16,22</sup> are 4900, 19 800, and 30 100, respectively. Figures 1(g)–1(i) show the cavity's response in transmission with QDs with corresponding  $Q_{i+p} = 4500, 23\,200, \text{ and } 29\,500$ . For these low QD densities, the variation in the extracted  $Q_{i+p}$  due to differences in taper position is greater than the loss induced by QD absorption, at least up to  $Q_{i+p} \approx 3 \times 10^4$ . The ability to maintain high- $Q$  in the presence of the QDs is promising for a number of potential applications, such as single QD cQED and low-threshold microcavity lasers.

For PL measurements, a 980 nm diode laser is coupled through a variable optical attenuator into the fiber taper, which is brought into contact with the devices. The transmitted signal is then directed through a long pass 1064 nm filter and into a grating spectrometer coupled with a liquid  $N_2$  cooled InGaAs array. Spectra are recorded with a 180 s integration time under a typical excitation power of  $100 \mu\text{W}$ . PL spectra from each cavity are shown in Fig. 2, including another mode in the MH cavity that did not appear in transmission [Fig. 2(c)]. The  $Q$  factors observed in PL are consistent with those seen in transmission measurements, though our spectral resolution is limited to  $\approx 0.09$  nm. We note that the cavity modes operate on the long wavelength tail-end of the QD distribution, as seen in the reference PL spectrum shown in the inset of Fig. 2(a) for an ensemble of QDs not in a cavity. This suggests the number of QDs interacting with the cavity modes may be significantly reduced with respect to the number that physically reside in the cavity, though a

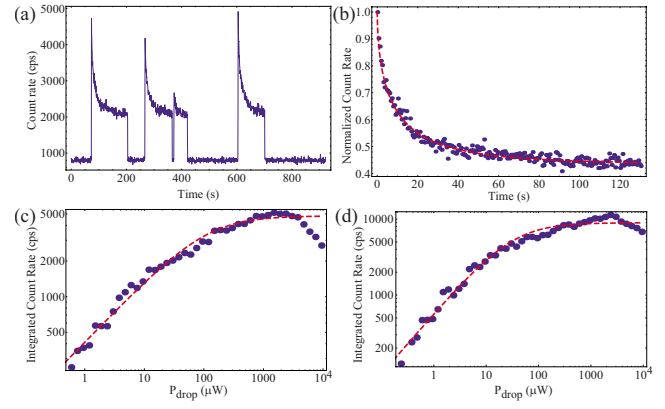


FIG. 3. (Color online) (a) Continuous measurement of PL on an SPCM while the excitation is intermittently turned off and on. (b) Close-up of one of the photodarkening curves taken in (a) along with fit (dashed). [(c) and (d)] PL saturation measurements of the modes at 1522.7 and 1532.1 nm in the MH cavity with fits (dashed).

measurement of the QD homogeneous linewidth is needed to confirm this.

Using the transmission measurements in Fig. 1, we can estimate the efficiency  $\eta_o$  with which a cavity photon out-couples into the fiber taper. A QD's out-coupling efficiency would then be the product of  $\eta_o$  with the fraction of QD radiation into the cavity mode.  $\eta_o$  is estimated<sup>16,22</sup> from the on-resonance transmission level  $T_{\text{res}}$  as  $\eta_o = (1 - \sqrt{T_{\text{res}}})/2$  where  $\eta_o$  represents collection in transmission. For the H1 cavity in Fig. 1(g),  $T_{\text{res}} = 0.381$  so that  $\eta_o = 19.1\%$ . A similar efficiency ( $T_{\text{res}} = 0.562$  and  $\eta_o = 12.5\%$ ) has been measured when the taper is in contact with the L3 cavity [inset of Fig. 2(b)], while coupling to the MH cavity as shown in Fig. 1(i) yields a somewhat smaller value ( $T_{\text{res}} = 0.670$  and  $\eta_o = 9.07\%$ ); fluctuations in the detected signal result in uncertainties in  $\eta_o$  of  $\leq 0.1\%$ . These results generally compare favorably to calculated free-space collection efficiencies of  $\approx 10\%$  using high numerical aperture objectives,<sup>23</sup> with the added advantage of direct collection into a single mode optical fiber.

Our experimental configuration also enabled measurement of photodarkening behavior previously observed in PbS QDs.<sup>21</sup> In this case, PL from the MH cavity is directed through long pass filters at 1064 and 1400 nm and detected at an InGaAs single photon counting module (SPCM) (Ref. 10) with 2.5 ns gate width, 20% detection efficiency, and 5  $\mu\text{s}$  dead time. As shown in Fig. 3(a), the PL is monitored continuously with a 0.6 s integration time while the 980 nm excitation source is turned on ( $P_{\text{drop}} = 154.0 \mu\text{W} \pm 9.5 \mu\text{W}$ ) and off. The PL clearly decays with time and requires an off time of at least 150 s to completely recover. This kind of photodarkening has been attributed to an average of single particle blinking where the overall ensemble PL decreases with time due to increasing numbers of emitters transitioning to a long-lived dark state.<sup>24–26</sup> Figure 3(b) shows a normalized photodarkening trace taken under the same excitation conditions as in Fig. 3(a). The data has been fit with a stretched exponential,<sup>26</sup>  $I(t) = I_{\text{eq}} + (1 - I_{\text{eq}}) \exp[-(t/T_o)^\alpha]$ , yielding fit parameters with 95% confidence intervals  $I_{\text{eq}} = 0.435 \pm 0.006$ ,  $T_o = 8.84 \pm 0.54$ , and  $\alpha = 0.57 \pm 0.38$ . While the fit parameters  $T_o$  and  $\alpha$  are consistent with literature,<sup>26</sup> the actual physical parameters associated with QD blinking can only be determined with further

single QD measurements beyond the scope of this work. However,  $I_{\text{eq}}$  is directly related to the ratio of average time spent in the dark state to the bright state, which for our QDs computes to a value of  $1.30 \pm 0.03$ . Short-timescale photodarkening and the difficulties associated with detection at  $1.55 \mu\text{m}$  make low density QD measurements that much more challenging.

The final experiment we performed was a saturation spectroscopy measurement of the two modes of the MH cavity. In this measurement, a PL spectrum was recorded (60 s integration) as the dropped excitation power was increased over more than four decades. To avoid photodarkening effects, the excitation was blocked for 30 s after each measurement and the spectrum was taken only after the excitation had been on for 30 s. Two Lorentzians were fit to each spectrum and the integrated count rate under each peak is plotted as a function of dropped power in Figs. 3(c) and 3(d). Each of these curves was fit to a two-level saturation with an adjustable power dependence,  $I(P) = A[P/(P + P_{\text{sat}})]^b$ . Interestingly, the saturation curves display a clear sublinear dependence on the dropped power below saturation. The mode at 1522.7 nm (1532.1 nm) fits to a value of  $b = 0.518 \pm 0.046$  ( $b = 0.795 \pm 0.082$ ). This sublinear dependence could be symptomatic of the trapped states associated with blinking.<sup>27</sup> The saturation curves are truncated due to heating in the tapered fiber and in the Si at excitation powers near 2 mW as evidenced by few nanometer redshifts in the cavity modes. Nonetheless, the saturation power can still be extracted from the data, albeit with a large uncertainty. We fit to  $P_{\text{sat}} = 153.2 \mu\text{W} \pm 65.3 \mu\text{W}$  ( $P_{\text{sat}} = 42.6 \mu\text{W} \pm 17.2 \mu\text{W}$ ) for the mode at 1522.7 nm (1532.1 nm). For a single PbS QD with absorption cross-section<sup>28</sup>  $\sigma = 4.59 \times 10^{-16} \text{ cm}^2$  and room-temperature excited state lifetime of  $\approx 100 \text{ ns}$ ,<sup>8</sup> the expected saturation excitation power for our tapered fiber setup is  $\approx 22 \mu\text{W}$ . Because the cross-section is so low, a nondiminished pump approximation is valid and the single particle saturation power should be accurate for small QD densities. Given the uncertainties in the fits as well as in the values for the cross-section and lifetime, the extracted saturation powers seem quite reasonable.

In conclusion, we have performed spectroscopy of  $1.55 \mu\text{m}$  PbS QDs dried on Si PCCs using a fiber taper waveguide. Future experiments will build toward single QD spectroscopy by lowering the QD density and improving the radiative efficiency by working in cryogenic conditions<sup>8</sup> and/or using brighter and more stable colloidal QDs.<sup>29</sup> A combination of these strategies will lead to the development of useful active nanophotonic devices in the telecommunications band.

The authors acknowledge fabrication support from D. L. Kwong and M. Yu at the Institute of Microelectronics in Singapore, useful discussions with Marcelo Davanço at NIST, funding support from NSF under Grant No. ECCS 0747787, the Nanoscale Science and Engineering Initiative under NSF Award No. CHE-0641523, and the New York State Office of Science, Technology, and Innovation.

- <sup>1</sup>Y. Akahane, T. Asano, B.-S. Song, and S. Noda, *Nature (London)* **425**, 944 (2003).
- <sup>2</sup>K. Srinivasan, P. E. Barclay, M. Borselli, and O. Painter, *Phys. Rev. B* **70**, 081306(R) (2004).
- <sup>3</sup>B.-S. Song, S. Noda, T. Asano, and Y. Akahane, *Nature Mater.* **4**, 207 (2005).
- <sup>4</sup>A. Polman, *J. Appl. Phys.* **82**, 1 (1997).
- <sup>5</sup>H. Park, A. Fang, S. Kodama, and J. Bowers, *Opt. Express* **13**, 9460 (2005).
- <sup>6</sup>F. Wise, *Acc. Chem. Res.* **33**, 773 (2000).
- <sup>7</sup>E. H. Sargent, *Adv. Mater. (Weinheim, Ger.)* **17**, 515 (2005).
- <sup>8</sup>M. T. Rakher, C. W. Wong, and K. Srinivasan (unpublished).
- <sup>9</sup>J. S. Steckel, S. Coe-Sullivan, V. Bulović, and M. G. Bawendi, *Adv. Mater. (Weinheim, Ger.)* **15**, 1862 (2003).
- <sup>10</sup>G. Ribordy, N. Gisin, O. Guinnard, D. Stuck, M. Wegmuller, and H. Zbinden, *J. Mod. Opt.* **51**, 1381 (2004).
- <sup>11</sup>I. Fushman, D. Englund, and J. Vuckovic, *Appl. Phys. Lett.* **87**, 241102 (2005).
- <sup>12</sup>R. Bose, X. Yang, R. Chatterjee, J. Gao, and C. W. Wong, *Appl. Phys. Lett.* **90**, 111117 (2007).
- <sup>13</sup>Z. Wu, Z. Mi, P. Bhattacharya, T. Zhu, and J. Xu, *Appl. Phys. Lett.* **90**, 171105 (2007).
- <sup>14</sup>A. G. Pattantyus-Abraham, H. Qiao, J. Shan, K. A. Abel, T.-S. Wang, F. C. J. M. van Veggel, and J. F. Young, *Nano Lett.* **9**, 2849 (2009).
- <sup>15</sup>R. Bose, J. F. McMillan, J. Gao, and C. W. Wong, *Appl. Phys. Lett.* **95**, 131112 (2009).
- <sup>16</sup>S. M. Spillane, T. J. Kippenberg, O. J. Painter, and K. J. Vahala, *Phys. Rev. Lett.* **91**, 043902 (2003).
- <sup>17</sup>K. Srinivasan and O. Painter, *Nature (London)* **450**, 862 (2007).
- <sup>18</sup>Purchased from Evident Technologies and identified in this paper to foster understanding, without implying recommendation or endorsement by NIST.
- <sup>19</sup>M. A. Hines and G. D. Scholes, *Adv. Mater. (Weinheim, Ger.)* **15**, 1844 (2003).
- <sup>20</sup>O. Painter, R. K. Lee, A. Yariv, A. Scherer, J. D. O'Brien, P. D. Dapkus, and I. Kim, *Science* **284**, 1819 (1999).
- <sup>21</sup>J. J. Peterson and T. D. Krauss, *Phys. Chem. Chem. Phys.* **8**, 3851 (2006).
- <sup>22</sup>P. Barclay, K. Srinivasan, and O. Painter, *Opt. Express* **13**, 801 (2005).
- <sup>23</sup>N.-V.-Q. Tran, S. Combrié, and A. D. Rossi, *Phys. Rev. B* **79**, 041101 (2009).
- <sup>24</sup>I. Chung and M. G. Bawendi, *Phys. Rev. B* **70**, 165304 (2004).
- <sup>25</sup>M. Pelton, D. G. Grier, and P. Guyot-Sionnest, *Appl. Phys. Lett.* **85**, 819 (2004).
- <sup>26</sup>J. Tang and R. A. Marcus, *J. Chem. Phys.* **123**, 204511 (2005).
- <sup>27</sup>V. Babentsov, J. Riegler, J. Schneider, M. Fiederle, and T. Nann, *J. Phys. Chem. B* **109**, 15349 (2005).
- <sup>28</sup>L. Cademartiri, E. Montanari, G. Calestani, A. Migliori, A. Guagliardi, and G. A. Ozin, *J. Am. Chem. Soc.* **128**, 10337 (2006).
- <sup>29</sup>J. M. Pietryga, D. J. Werder, D. J. Williams, J. L. Casson, R. D. Schaller, V. I. Klimov, and J. A. Hollingsworth, *J. Am. Chem. Soc.* **130**, 4879 (2008).